Claudin-5–siRNA transfected or control-siRNA transfected LECs also were cultured on the fibronectin-coated surface of 0.4-μm pore size tissue culture inserts for 2 days, followed by incubation in serum-free EBM for 24 hours. Then, fluorescein isothiocyanate was added to the upper chambers and the concentration of fluorescein isothiocyanate in the lower chambers was measured. All studies were performed in triplicate. Statistical analyses were performed using the unpaired Student's *t*-test.

Results

Edema Formation and Inflammation Induced by Acute UVB Irradiation Are Attenuated in K14-Ang1 Mice

To determine the role of Ang1 in cutaneous inflammation, K14-Ang1 mice and WT mice were exposed to 200 mJ/cm^2 of UVB irradiation. Pronounced ear swelling was observed in WT mice, starting at day 2 after UVB irradiation; however, the ear swelling was attenuated significantly in K14-Ang1 mice (Figure 1A). Histologic analysis revealed no major physiological difference between WT mice and K14-Ang1 mice in the absence of UVB exposure (Figure 1, B and C). The ears of UVB-irradiated WT mice showed the characteristics of inflammation, such as epidermal hyperplasia and dermal edema, whereas these changes were ameliorated in K14-Ang1 mice (Figure 1, D and E). Immunohistochemical analysis of a monocyte-macrophage marker, CD11b, indicated marked macrophage infiltration in UVB-exposed WT mouse ear, whereas the number of infiltrated macrophages was decreased in K14-Ang1 mice (Figure 1, H and I). Few or no CD11b-positive macrophages were found in WT or K14-Ang1 mice not exposed to UVB (Figure 1, F and G).

Promotion of Lymphatic and Blood Vascular Function of K14-Ang1 Mice during Inflammation

First, a Miles assay was performed to determine the effects of Ang1 on blood vessels. UVB exposure induced marked leakage of Evans blue dye in WT mice, whereas K14-Ang1 mice showed decreased leakiness, as compared with WT mice (Figure 2A). Quantitative analysis showed that UVB irradiation strongly enhanced dye leakage in WT mouse ear, whereas the increase of dye leakage was inhibited markedly in UVB-irradiated K14-Ang1 mice, although there was still a significant difference between nonirradiated and UVB-irradiated K14-Ang1 mice

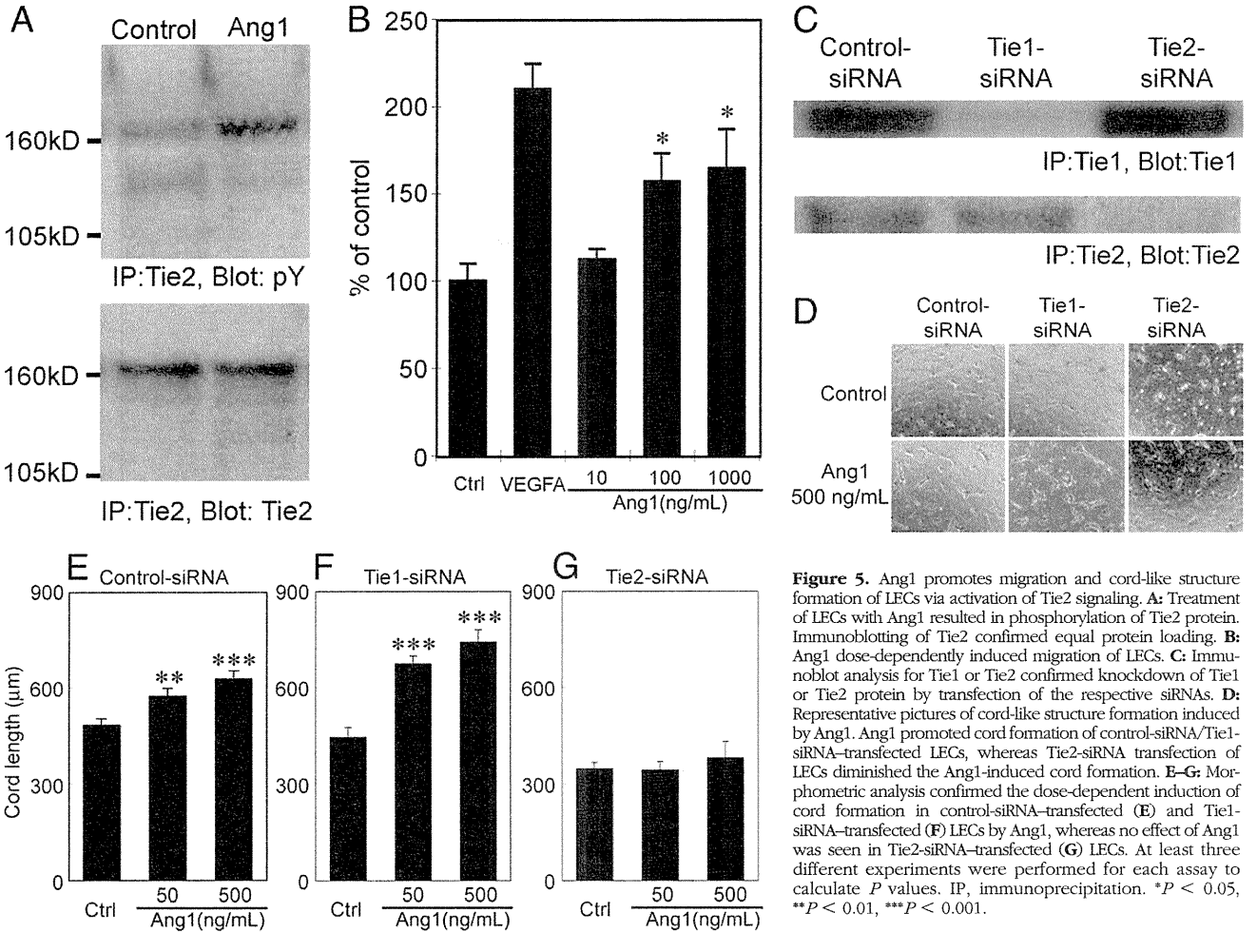

Figure 5. Ang1 promotes migration and cord-like structure formation of LECs via activation of Tie2 signaling. **A:** Treatment of LECs with Ang1 resulted in phosphorylation of Tie2 protein. Immunoblotting of Tie2 confirmed equal protein loading. **B:** Ang1 dose-dependently induced migration of LECs. **C:** Immunoblot analysis for Tie1 or Tie2 confirmed knockdown of Tie1 or Tie2 protein by transfection of the respective siRNAs. **D:** Representative pictures of cord-like structure formation induced by Ang1. Ang1 promoted cord formation of control-siRNA/Tie1-siRNA–transfected LECs, whereas Tie2-siRNA transfection of LECs diminished the Ang1-induced cord formation. **E–G:** Morphometric analysis confirmed the dose-dependent induction of cord formation in control-siRNA–transfected (**E**) and Tie1-siRNA–transfected (**F**) LECs by Ang1, whereas no effect of Ang1 was seen in Tie2-siRNA–transfected (**G**) LECs. At least three different experiments were performed for each assay to calculate *P* values. IP, immunoprecipitation. $^*P < 0.05$, $^{**}P < 0.01$, $^{***}P < 0.001$.

(Figure 2B). Next, to visualize lymphatic function, Evans blue dye was injected intradermally into mouse ear. Lymph leakage was found in the whole ear of UVB-irradiated WT mice at 5 and 10 minutes after dye injection as previously described,[8] whereas lymphatic vessels of UVB-exposed K14-Ang1 mice were still visible at 5 and 10 minutes after dye injection, indicating that the increase of lymphatic capillary permeability was attenuated in K14-Ang1 mice. Moreover, at 1 minute after dye injection, dye spots were found close to the branching points of lymphatic vessels only in UVB-irradiated WT mice, suggesting the presence of abnormal and leaky collecting vessels (Figure 2C). In contrast, in non-UV, there was no significant difference between WT mice and K14-Ang1 in terms of lymph leakage at 5 minutes after dye injection, however, at 10 minutes, K14-Ang1 mouse ears showed inhibited lymph leakage as compared with WT mice.

Double-immunofluorescence analysis using antibodies for blood vessel–specific antigen, panendothelial antigen-1,[21] and a lymphatic specific marker, LYVE-1, was performed. UVB induced marked enlargement of LYVE-1–positive lymphatic vessels in WT mice as compared with ear skin not exposed to UVB (Figure 3, A and C), whereas in K14-Ang1 mice, the enlargement of lymphatic vessels and blood vessels after UVB was attenuated, as compared with WT. In contrast, the density of lymphatic vessels was increased in K14-Ang1 mice compared with WT mice (Figure 3, B and D). Morphometric analysis of lymphatic vessels using IP-LAB software showed an increase in the average size of the inflamed lymphatic vessels of WT mice as compared with the vessels of nonirradiated WT mice, although no significant difference was found in the vessel density. As we had expected, the average size of lymphatic vessels was decreased in K14-Ang1 mice after UVB irradiation. In contrast, the density of lymphatic vessels was increased in K14-Ang1 mice, as compared with WT mice (Figure 3, E and F). To analyze if the increased area of lymphatic vessels in K14-Ang1 mice resulted from the presence of more lymphatic endothelial cells, double-immunofluorescence analysis for podoplanin and a proliferation marker, Ki-67, was performed. The results showed that the number of Ki-67–positive cells was increased in K14-Ang1 mice as compared with WT mice (1.75 ± 0.96 cells/slide in K14-Ang1 mice and 0.25 ± 0.5 cells/slide in WT mice; $P = 0.016$) (Figure 3, G and H). Under physiological conditions, the size and density of blood vessels were increased in K14-Ang1 mice, as previously described (Figure 3, A and B).[14] After UVB irradiation, a relatively small change of blood vessel size was found in K14-Ang1 mice as compared with WT mice. The vessel density was comparable in skin exposed and not exposed to UVB (Figure 3, I and J).

Enhanced Lymphatic Integrity in Inflamed Ears of K14-Ang1 Mice

We previously found that the enlarged lymphatic vessels induced by UVB irradiation are leaky and hyperpermeable, suggesting that lymphatic function is impaired.[8] Therefore, we hypothesized that altered expression pattern of tight junction molecules might be associated with the leakiness of inflamed lymphatic vessels. To test this idea, we performed whole-mount staining for claudin-5 and/or podoplanin/CD31 in ears of animals exposed or not exposed to UVB irradiation. Interestingly, UVB irradiation led to the loss of claudin-5 protein, which was localized exclusively to cell–cell junctions at the tips of lymphatic capillaries without UVB, whereas claudin-5 expression already was redistributed at cell–cell junctions in UVB-irradiated K14-Ang1 mice (Figure 4A). Confocal

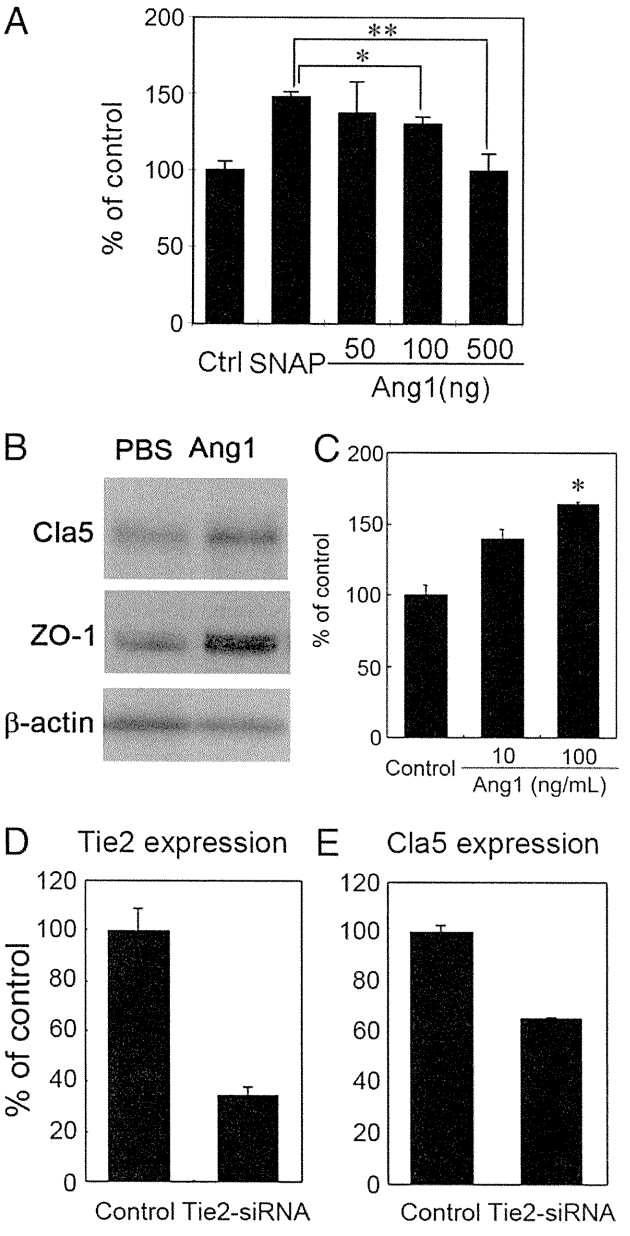

Figure 6. Ang1 promotes the integrity of LECs by increasing expression of tight junction molecules. **A:** Nitric oxide donor S-nitroso-N-acetylpenicillamine (SNAP) increased the lymphatic permeability, whereas co-incubation of LECs with Ang1 and SNAP dose-dependently inhibited the nitric oxide–induced hyperpermeability of LECs. **B:** Treatment with Ang1 for 4 hours markedly increased the levels of tight junction molecules claudin-5 and ZO-1. β-Actin is shown as a loading control. **C:** Claudin-5 expression was dose-dependently increased in the presence of Ang1. (**D** and **E**) LECs transfected with Tie2-siRNA showed decreased expression of Tie2 (**D**) and claudin-5 (**E**). At least three different experiments were performed for each assay to calculate P values. $^{*}P < 0.05$, $^{**}P < 0.01$.

microscopy revealed that claudin-5 protein was present in the cellular membrane of collecting lymphatic vessels in skin, whereas its expression was diminished in inflamed skin (Figure 4B). These data suggested that the lymphatic capillaries and collecting vessels became leaky after UVB irradiation because of loss of claudin-5.

Next, to determine the expression pattern of the lymphatics in K14-Ang1 mice, immunofluorescence analyses using antibodies for the endothelial tight junction molecule claudin-5 and lymphatic vessels were performed. Double-immunofluorescence analysis using antibodies against podoplanin and claudin-5 also confirmed that UVB irradiation resulted in the loss of claudin-5 expression at cellular membranes of lymphatic vessels in WT mice. Moreover, loss of claudin-5 in lymphatics of UVB-irradiated WT mice (Figure 4D), already was redistributed in cell–cell junctions of K14-Ang1 mice (Figure 4E). Another tight junction molecule, ZO-1, also was expressed in podoplanin-positive lymphatic vessels. Double-immunofluorescence staining for podoplanin and ZO-1 showed that ZO-1 expression in lymphatic vessels was lost in the UVB-irradiated skin of WT mice, and the level was markedly less than that in UVB-exposed K14-Ang1 mice. These data indicate that the lymphatic integrity of inflamed skin of UVB-exposed K14-Ang1 mice was enhanced, as compared with WT.

Tie2 Activation by Ang1 Induces Cell Migration and Cord Formation in Vitro

To examine the role of Tie2 signaling in LECs, immunoblot analysis was performed after immunoprecipitation of Tie2. In the presence of Ang1, pronounced Tie2 phosphorylation was found as compared with the control cells, although immunoblot analysis of Tie2 protein confirmed equal loading of protein (Figure 5A). Next, we investigated the effect of Ang1 on LECs. Treatment of LECs with Ang1 dose-dependently induced migration (Figure 5B). The effect of VEGF-A also was assessed as a positive control. Further, Ang1 dose-dependently promoted cord formation of LECs. Our results are consistent with a previous finding of Tie1 phosphorylation of LECs in the presence of Ang1.

To determine which pathway is critical in the mediation of Ang1 signaling of LECs, the Tie2 or Tie1 receptor was specifically knocked down by the transfection of silencer RNAs. We confirmed specific knockdown of Tie1 or Tie2 expression by immunoblotting (Figure 5C). In addition, a cord-formation assay of these cells was performed. Ang1 promoted cord formation of Tie1-knockdown cells as well as control siRNA-transfected cells, whereas in cells transfected with siRNA of Tie2, the effect of Ang1 was reduced, showing the importance of Ang1/Tie2 signaling in LECs (Figure 5, D–G).

Ang1 Enhances Lymphatic Integrity by Increasing Levels of Tight Junction Molecules in Vitro

In vivo, K14-Ang1 mice showed increased levels of tight junction molecules in inflamed skin. To analyze the contribution of Ang1/Tie2 signaling to lymphatic integrity, a Transwell permeability assay was performed in the presence or absence of Ang1 together with a nitric oxide donor, S-nitroso-N-acetylpenicillamine.[20] Ang1 dose-dependently inhibited the lymphatic permeability (Figure 6A). Furthermore, we detected increased expression of claudin-5 as well as ZO-1 after the addition of Ang1, whereas β-actin expression was similar in the two groups (Figure 6B). Moreover, Ang1 treatment of LECs dose-dependently enhanced the expression of claudin-5 (Figure 6C), suggesting that Ang1 induces an increase of lymphatic integrity by promoting expression of tight junction molecules. In contrast, the transfection of LECs with siRNA-Tie2 decreased claudin-5 expression (Figure 6, D and E). These data indicate that Ang1/Tie2 signaling influences lymphatic permeability by modulating expression of tight junction molecules.

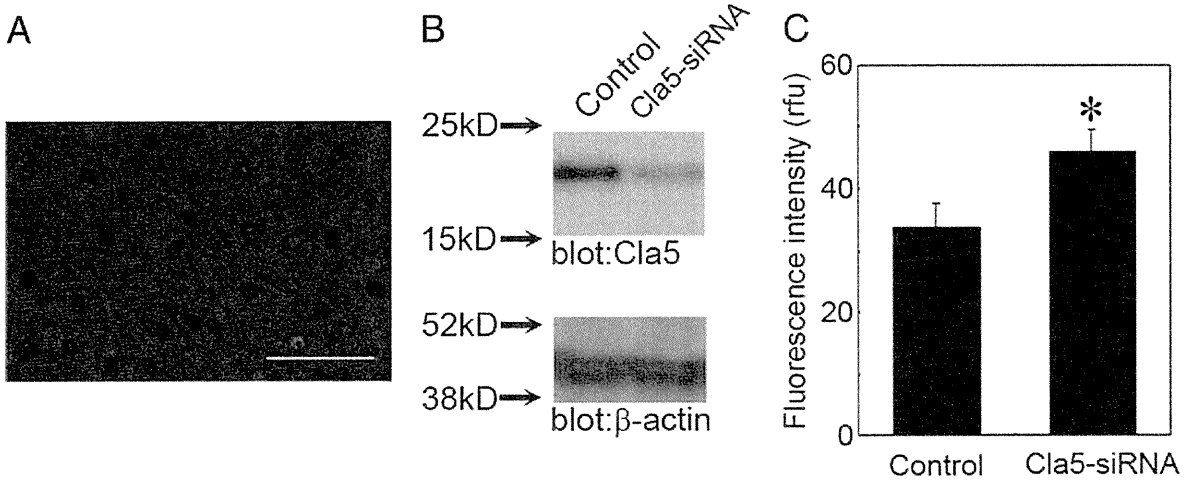

Figure 7. Claudin-5 regulates lymphatic integrity *in vitro*. **A:** Immunofluorescence of LECs for claudin-5 (red) confirmed the expression of claudin-5 on the cellular membrane of LECs. **B:** Western blot analyses revealed a significant decrease of claudin-5 protein in the presence of claudin-5–specific siRNA, whereas β-actin protein levels were comparable in LECs transfected with scramble-siRNA and with claudin-5 siRNA. **C:** Claudin-5 siRNA transfection resulted in increased permeability of LECs *in vitro*. Three different experiments were performed for each assay. $^*P < 0.001$. Scale bar = 100 μm.

Claudin-5 Influences Lymphatic Permeability

Claudin-5 expression was increased in the cellular membrane of lymphatic endothelial cells *in vitro* (Figure 7A). To elucidate claudin-5 function in LECs, claudin-5 expression was knocked down with claudin-5 siRNA; β-actin expression remained similar in the control and claudin-5 siRNA transfectants (Figure 7B). Claudin-5 knockdown resulted in increased permeability of LECs *in vitro* (Figure 7C).

Discussion

Complex phenomena occur during skin inflammation, including epidermal hyperplasia, erythema, edema formation, vessel dilation, and infiltration of inflammatory cells.[1] It also has been shown that lymphatic function actively participates in the resolution of inflammation by modulating lymphangiogenic factors, VEGF-A and VEGF-C/D, secreted from macrophages.[4] In our skin inflammation model, the subcutaneous delivery of VEGF-C attenuated skin inflammation by promoting lymphangiogenesis.[6] In contrast, VEGF-A up-regulation in keratinocytes triggered lymphatic impairment, whereas systemic blockade of VEGF-A attenuated skin inflammation by inhibiting the enlargement of lymphatic vessels.[8] These data indicate that lymphangiogenic factors could play distinct roles in inflammation resolution.

Our results showed that activation of Ang1/Tie2 signaling attenuated inflammation by promoting lymphatic integrity, as well as inhibiting blood vascular hyperpermeability in inflamed tissue. Blood vessels of K14-Ang1 mice were shown to be resistant to leakage induced by an inflammatory stimulus.[22] Therefore, the effect of Ang1 on blood vessels may contribute to the attenuation of inflammation in K14-Ang1 mice. Recently, Ang1 was shown to promote lymphatic formation and hyperplasia.[9,10] We also confirmed increased lymphatic density in the skin of K14-Ang1 mice as compared with WT mice under physiological conditions. Interestingly, the enlargement of lymphatic vessels in inflamed skin of UVB-exposed K14–Ang1 mice was reduced, compared with UVB-exposed WT mice. Furthermore, intravital lymphangiography by injection of Evans blue dye into the ear of UVB-exposed K14-Ang1 mice indicated that the increase of lymphatic permeability also is reduced in these mice. Unlike VEGF-C, Ang1 had no effect on proliferation of lymphatic endothelial cells *in vitro* (data not shown), although Ang1 dose-dependently promoted cell migration and cord formation. Taken together, these results indicate that, in addition to the well-known effect of Ang1 on blood vessels in inflammation,[23] Ang1 has a distinctive functional role in lymphatic vessels of inflamed tissue, serving to modulate lymphatic integrity.

How is lymphatic integrity regulated in inflammation? Lymphatic hyperplasia, together with lymphatic enlargement, is found in several models of inflammation.[3,12] Surprisingly, loss of the tight junction molecule claudin-5 was found in inflamed lymphatic capillaries, as well as collecting vessels. In inflamed skin, lymphatic vessels could be pulled open by anchoring filaments that connect lymphatic endothelial cells with elastic fibers in the extracellular matrix, presumably to wash out increased interstitial tissue fluid resulting from the increased vascular permeability.[24] However, overextension of lymphatic endothelial cells also can cause edema formation.[25] Our results showed that overextension of lymphatic endothelial cells in capillaries as well as collecting vessels was caused by loss of tight junction molecules, claudin-5 and ZO-1 at cell–cell junctions, resulting in lymphatic impairment and prolonged edema and inflammation.

Recent results have indicated that VEGF-A induces disruption of claudin-5 in the blood-brain barrier.[26] Further, up-regulation of VEGF-A was detected in keratinocytes after UVB exposure *in vitro* as well as *in vivo*, and VEGF-A was identified as a mediator of skin inflammation after UVB exposure.[15,27] It would be of interest to see if VEGF-A up-regulation after UVB also mediates decreased expression of tight junction proteins in lymphatic vessels, followed by lymphatic impairment in inflamed skin. Furthermore, we found that activation of Ang1/Tie2 signaling increased the TJPs *in vivo* and *in vitro*. Adrenomedullin has been shown to control murine lymphatic development by stabilizing the lymphatic endothelial barrier,[28,29] and its receptor-modulator, receptor activity modifying protein–2 (RAMP2), modulated vascular integrity in mice.[30] We also confirmed that an endothelial-specific TJP, claudin-5, is a key modulator of the lymphatic endothelial barrier *in vitro*. However, in contrast to adrenomedullin, no obvious change of TJPs was found in K14-Ang1 mice under physiological conditions *in vivo*, whereas inflamed lymphatic vessels showed TJPs at cell–cell junctions *in vivo*, suggesting a distinct role of Ang1/Tie2 signaling in maintaining the lymphatic integrity of inflamed tissue.

In conclusion, we have identified a regulatory pathway that serves to maintain lymphatic integrity during inflammation by controlling TJP components. Ang1, or small molecules that directly activate Tie2, may have potential for the treatment of lymphatic dysfunction during inflammation.

Acknowledgments

We thank Koji Aruga, Fumika Miyohashi, and Junko Yamane for their technical assistance.

References

1. Cueni LN, Detmar M: New insights into the molecular control of the lymphatic vascular system and its role in disease. J Invest Dermatol 2006, 126:2167–2177
2. Tammela T, Alitalo K: Lymphangiogenesis: molecular mechanisms and future promise. Cell 2010, 140:460–476
3. Baluk P, Tammela T, Ator E, Lyubynska N, Achen MG, Hicklin DJ, Jeltsch M, Petrova TV, Pytowski B, Stacker SA, Yla-Herttuala S, Jackson DG, Alitalo K, McDonald DM: Pathogenesis of persistent lymphatic vessel hyperplasia in chronic airway inflammation. J Clin Invest 2005, 115:247–257
4. Kataru RP, Jung K, Jang C, Yang H, Schwendener RA, Baik JE, Han SH, Alitalo K, Koh GY: Critical role of CD11b+ macrophages and

VEGF in inflammatory lymphangiogenesis, antigen clearance, and inflammation resolution. Blood 2009, 113:5650–5659
5. Alitalo K, Tammela T, Petrova TV: Lymphangiogenesis in development and human disease. Nature 2005, 438:946–953
6. Kajiya K, Sawane M, Huggenberger R, Detmar M: Activation of the VEGFR-3 pathway by VEGF-C attenuates UVB-induced edema formation and skin inflammation by promoting lymphangiogenesis. J Invest Dermatol 2009, 129:1292–1298
7. Nagy JA, Vasile E, Feng D, Sundberg C, Brown LF, Detmar MJ, Lawitts JA, Benjamin L, Tan X, Manseau EJ, Dvorak AM, Dvorak HF: Vascular permeability factor/vascular endothelial growth factor induces lymphangiogenesis as well as angiogenesis. J Exp Med 2002, 196:1497–1506
8. Kajiya K, Hirakawa S, Detmar M: Vascular endothelial growth factor-a mediates ultraviolet B-induced impairment of lymphatic vessel function. Am J Pathol 2006, 169:1496–1503
9. Morisada T, Oike Y, Yamada Y, Urano T, Akao M, Kubota Y, Maekawa H, Kimura Y, Ohmura M, Miyamoto T, Nozawa S, Koh GY, Alitalo K, Suda T: Angiopoietin-1 promotes LYVE-1-positive lymphatic vessel formation. Blood 2005, 105:4649–4656
10. Tammela T, Saaristo A, Lohela M, Morisada T, Tornberg J, Norrmen C, Oike Y, Pajusola K, Thurston G, Suda T, Yla-Herttuala S, Alitalo K: Angiopoietin-1 promotes lymphatic sprouting and hyperplasia. Blood 2005, 105:4642–4648
11. Augustin HG, Koh GY, Thurston G, Alitalo K: Control of vascular morphogenesis and homeostasis through the angiopoietin-Tie system. Nat Rev Mol Cell Biol 2009, 10:165–177
12. Baluk P, Fuxe J, Hashizume H, Romano T, Lashnits E, Butz S, Vestweber D, Corada M, Molendini C, Dejana E, McDonald DM: Functionally specialized junctions between endothelial cells of lymphatic vessels. J Exp Med 2007, 204:2349–2362
13. Nitta T, Hata M, Gotoh S, Seo Y, Sasaki H, Hashimoto N, Furuse M, Tsukita S: Size-selective loosening of the blood-brain barrier in claudin-5-deficient mice. J Cell Biol 2003, 161:653–660
14. Suri C, McClain J, Thurston G, McDonald DM, Zhou H, Oldmixon EH, Sato TN, Yancopoulos GD: Increased vascularization in mice overexpressing angiopoietin-1. Science 1998, 282:468–471
15. Yano K, Kajiya K, Ishiwata M, Hong YK, Miyakawa T, Detmar M: Ultraviolet B-induced skin angiogenesis is associated with a switch in the balance of vascular endothelial growth factor and thrombospondin-1 expression. J Invest Dermatol 2004, 122:201–208
16. Kidoya H, Naito H, Takakura N: Apelin induces enlarged and nonleaky blood vessels for functional recovery from ischemia. Blood 2010, 115:3166–3174
17. Hirakawa S, Fujii S, Kajiya K, Yano K, Detmar M: Vascular endothelial growth factor promotes sensitivity to ultraviolet B-induced cutaneous photodamage. Blood 2005, 105:2392–2399
18. Hirakawa S, Hong YK, Harvey N, Schacht V, Matsuda K, Libermann T, Detmar M: Identification of vascular lineage-specific genes by transcriptional profiling of isolated blood vascular and lymphatic endothelial cells. Am J Pathol 2003, 162:575–586
19. Kajiya K, Hirakawa S, Ma B, Drinnenberg I, Detmar M: Hepatocyte growth factor promotes lymphatic vessel formation and function. EMBO J 2005, 24:2885–2895
20. Kajiya K, Huggenberger R, Drinnenberg I, Ma B, Detmar M: Nitric oxide mediates lymphatic vessel activation via soluble guanylate cyclase alpha1beta1-impact on inflammation. FASEB J 2008, 22: 530–537
21. Liersch R, Nay F, Lu L, Detmar M: Induction of lymphatic endothelial cell differentiation in embryoid bodies. Blood 2006, 107: 1214–1216
22. Thurston G, Suri C, Smith K, McClain J, Sato TN, Yancopoulos GD, McDonald DM: Leakage-resistant blood vessels in mice transgenically overexpressing angiopoietin-1. Science 1999, 286:2511–2514
23. Fiedler U, Augustin HG: Angiopoietins: a link between angiogenesis and inflammation. Trends Immunol 2006, 27:552–558
24. Gerli R, Solito R, Weber E, Agliano M: Specific adhesion molecules bind anchoring filaments and endothelial cells in human skin initial lymphatics. Lymphology 2000, 33:148–157
25. Skobe M, Detmar M: Structure, function, and molecular control of the skin lymphatic system. J Investig Dermatol Symp Proc 2000, 5:14–19
26. Argaw AT, Gurfein BT, Zhang Y, Zameer A, John GR: VEGF-mediated disruption of endothelial CLN-5 promotes blood-brain barrier breakdown. Proc Natl Acad Sci U S A 2009, 106:1977–1982
27. Yano K, Kadoya K, Kajiya K, Hong YK, Detmar M: Ultraviolet B irradiation of human skin induces an angiogenic switch that is mediated by upregulation of vascular endothelial growth factor and by downregulation of thrombospondin-1. Br J Dermatol 2005, 152:115–121
28. Dunworth WP, Fritz-Six KL, Caron KM: Adrenomedullin stabilizes the lymphatic endothelial barrier in vitro and in vivo. Peptides 2008, 29:2243–2249
29. Fritz-Six KL, Dunworth WP, Li M, Caron KM: Adrenomedullin signaling is necessary for murine lymphatic vascular development. J Clin Invest 2008, 118:40–50
30. Ichikawa-Shindo Y, Sakurai T, Kamiyoshi A, Kawate H, Iinuma N, Yoshizawa T, Koyama T, Fukuchi J, Iimuro S, Moriyama N, Kawakami H, Murata T, Kangawa K, Nagai R, Shindo T: The GPCR modulator protein RAMP2 is essential for angiogenesis and vascular integrity. J Clin Invest 2008, 118:29–39

Int J Hematol (2012) 95:138–142
DOI 10.1007/s12185-012-1011-3

Involvement of non-vascular stem cells in blood vessel formation

Nobuyuki Takakura

Received: 4 January 2012 / Revised: 18 January 2012 / Accepted: 18 January 2012 / Published online: 4 February 2012

Abstract Blood vessels clearly act as conduits for blood flow, but recently the concept that they are also involved in organ maintenance, especially by providing a niche for organ-specific stem cells, has begun to emerge. Moreover, several lines of evidence suggest that hematopoietic stem cells can differentiate directly into cells composing blood vessels. Recently, cancer stem cells (CSCs) have also been assigned these roles in the cancer microenvironment. Although anti-angiogenic drugs have been developed and are utilized in the clinic for their anti-tumor activity, their suppressive effects on tumor growth have been disappointing. This may be caused by transferring drug resistance from CSCs to endothelial cells. It has been suggested that CSCs localize in the peri-vascular niche. Therefore, it is extremely important to know how the vascular niche maintains CSCs, as such knowledge may enable us to develop promising new approaches to cancer treatment.

Keywords Endothelial cells · Hematopoietic stem cells · Angiogenesis · Vasculogenic mimicry · Cancer stem cell

Introduction

Blood vessel formation takes place by two main processes [1]. "Vasculogenesis" is mainly observed in the embryo, where angioblasts derived from mesodermal cells give rise to endothelial cells (ECs) which form vascular tubes (Fig. 1). Blood vessels generated in this way are immature, but gradually mature via several additional processes collectively termed "remodeling." These include interactions of ECs with mural cells for stabilization of the new blood vessels, fusion of blood vessels resulting in bore enlargement, intussusceptions that increase vascular density, and regression of surplus vessels. The second main process, unlike vasculogenesis, results in the generation of new blood vessels from pre-existing vessels and is termed "angiogenesis" (Fig. 2a). Blood vessel formation is closely associated with the progression of many diseases, including cancer, retinopathy, inflammation, and atherosclerosis, which are classified as vascular diseases. Angiogenesis is the main contributor to new blood vessel formation in vascular diseases. For this reason, the mechanisms responsible for angiogenesis have been extensively analyzed at the molecular and cellular levels with the aim of developing novel strategies to regulate angiogenesis.

For the past two decades, investigations of the molecular mechanisms of blood vessel formation have focused especially on receptor tyrosine kinases, such as vascular endothelial growth factor (VEGF) receptors (VEGFR1, 2, and 3), platelet-derived growth factor (PDGF) receptor beta (PDGFRβ), and the Tie2 receptor for angiopoietin (Ang) [2]. VEGFs regulate development, tube formation, and proliferation of ECs, PDGF-BB induces recruitment of mural cells near ECs, the Tie2 agonist Ang1 mainly induces EC–EC and EC–mural cell adhesion for stabilization of blood vessels, and another Tie2 antagonist, Ang2, inhibits EC–mural cell adhesion, thereby enabling the initiation of sprouting angiogenesis. Prolonged dissociation of mural cells from ECs mediated by Ang2 also induces blood vessel regression. Efforts to target these pathways have resulted in the development of many VEGF/VEGFR inhibitors that are already utilized clinically [3].

N. Takakura (✉)
Department of Signal Transduction, Research Institute for Microbial Diseases, Osaka University, 3-1 Yamada-ka, Suita 565-0871, Japan
e-mail: ntakaku@biken.osaka-u.ac.jp

Angiogenesis inhibitors effectively prevent blood vessel formation and tumor growth in mouse models, but it is widely accepted that these drugs are not effective in humans when used individually as single agents. However, they do improve permeability by normalization of abnormally leaky blood vessels with the result that a combination of angiogenesis inhibitor with anti-cancer drugs does have an effect on tumor growth in humans [4]. Clinical application of angiogenesis inhibitors is of course usually aimed at disrupting the blood supply to tumors to starve them of nutrients and oxygen. If blood vessels cannot be destroyed by means of a strategy based on knowledge of physiological angiogenesis, it is clear that research on tumor-specific processes of blood vessel formation is required.

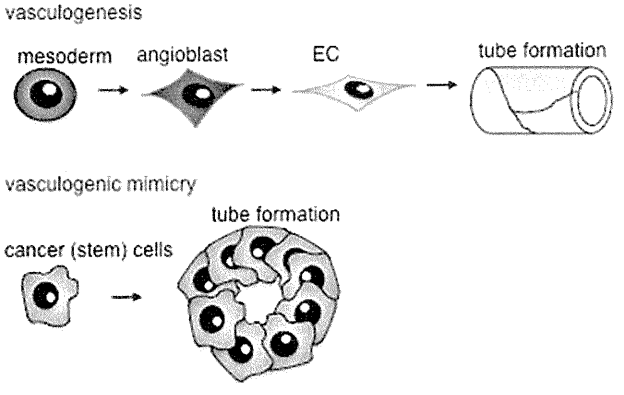

Fig. 1 Schema of vasculogenesis by endothelial cells (ECs) and vasculogenic mimicry by cancer (stem) cells. See text for details

Recently, several mechanisms indicating a direct contribution to blood vessel formation by cancer cells themselves, particularly cancer stem cells (CSCs), have been described [5, 6]. Here, we will review new data on the contribution of CSCs to blood vessel formation, in addition to the classical function of hematopoietic stem cells (HSC) in promoting angiogenesis.

Roles of hematopoietic stem cells in promoting blood vessel formation

Much attention has been focused on the source of ECs derived from bone marrow (BM; endothelial progenitor cells, the so-called "EPC"). These are characterized as non-hematopoietic immature ECs that can differentiate into mature ECs. However, it has also been reported that BM hematopoietic cells can act as a source of ECs as well. We have also determined that CD45-positive BM HSCs can differentiate into ECs [7]. Moreover, we found that HSCs in adult BM, as well as in the embryo, can transdifferentiate into mural cell populations via CD11b-positive myeloid progenitor cells (Fig. 2b). HSCs from mouse embryonic brain can differentiate into mural cells in vitro under the usual culture conditions in serum-containing media, without the addition of specific factors [7]. However, TGFβ stimulation is required for transdifferentiation of adult BM HSCs into mural cells. Recently, it was reported that conversion of ECs into mesenchymal stem cells can be induced by TGFβ or BMP4 [8]. Therefore, it is

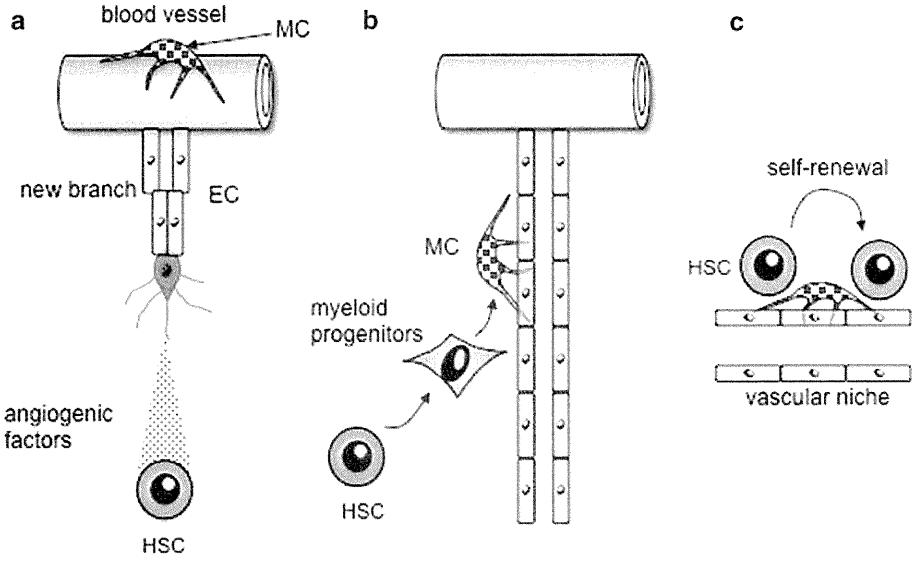

Fig. 2 Intimate interactions of hematopoietic stem cells with vascular cells. **a** In several situations, angiogenesis, new blood vessel formation from preexisting blood vessels, can be induced. During angiogenesis, hematopoietic stem cells (HSCs) produce angiogenic factors to induce angiogenesis by affecting proliferation and migration of endothelial cells (ECs). *MC* mural cells. **b** HSCs have the ability to differentiate into MCs via myeloid progenitors and thus to enhance the stability of newly developed blood vessels. **c** Vascular cells such as ECs and MCs support stemness of HSCs in the vascular niche

possible that the emergence of a mural cell population from HSCs is the result of differentiation of ECs derived from HSCs into mesenchymal stem cells. As previously suggested, Crisan et al. [9] recently showed that pericytes (mural cells observed in capillaries) expressing CD146, NG2, and PDGFRβ are mesenchymal stem cells possessing osteogenic, chondrogenic, and myogenic properties. It is possible that a certain population of pericytes is derived from HSCs.

AML1/Runx1 is a transcription factor required for the development of HSCs; AML1-deficient mice show complete lack of definitive (adult)-type HSCs. Abnormal blood vessel structure, and subsequently massive hemorrhage in the ventricles of the central nervous system, causes lethality in AML1 mutant embryos. Mural cell development in the brain of AML1 mutant embryos is deficient. In the brain of wild-type mice at the same stage, HSCs first appear in the parenchyma, adhere to ECs, and start to expressing smooth muscle actin, a marker of mural cells. Because we found that transdifferentiation of HSCs into mural cells was possible, we concluded that disruption of the blood vessels observed in AML mutant mice was caused by their instability due to the absence of mural cell development from HSCs. In terms of the biological significance of differentiation of HSCs into vascular cells, we failed to unequivocally demonstrate a crucial role for HSC-derived ECs, but we did show that mural cell-lineage cells physiologically derived from HSCs at least promote the maturation/stabilization of blood vessels [7].

Another role of HSCs in blood vessel formation is to guide the direction of migration of blood vessels sprouting from pre-existing vessels (Fig. 2a). Indeed, HSCs are frequent in peripheral blood and organs in adults as well as embryos. AML1-deficient mice also provide a good tool to analyze interactions between HSCs and ECs because the former are totally absent, as described above. We found that sprouting of capillaries generated during angiogenesis is retarded in the brain, pericardium, and other organs. During embryogenesis, HSCs migrate into the parenchyma of the brain first and subsequently ECs migrate toward the HSCs. We found that Ang1, which is produced in large amounts by HSCs, induces EC migration in vitro in the manner of a chemoattractant. Therefore, we concluded that Ang1 produced by HSCs stimulates Tie2 on ECs; this results in recruitment of ECs near HSCs, and thus in promotion of sprouting angiogenesis (Fig. 2a) [10]. The main role of HSCs remains the production of all types of mature hematopoietic cells, but another role for these cells may be in blood vessel formation closely associated with stem cell vascular niche formation, i.e., HSCs themselves generate their own niche for maintenance of stemness (Fig. 2c).

Vasculogenic mimicry

In less evolutionarily derived species, especially small animals, diffusion is sufficient for supplying fluids (carrying oxygen and nutrients) to all parts of the body. However, as body size increases, this becomes inefficient at supplying blood to all tissues and active pumping of some kind becomes a requirement. Moreover, the space between organs/tissues provides an initial space for development of tubes which formed an open circulatory system for blood flow coming from the heart. As far as we have been able to determine, in *Halocynthia roretzi* (the common sea squirt), there are no ECs in the space between organs but fluid from the heart flows through these spaces. Therefore, in this case at least, this space without ECs is indeed utilized in the same manner as blood vessels.

In mammals, blood vessel-like tubes as observed above are induced in the tumor environment. Maniotis et al. [11] reported that melanoma cells themselves generate tube-like structures which might be involved in microcirculation. They designated this process "vasculogenic mimicry" (Fig. 1). When typically highly invasive melanoma cells were cultured in three-dimensional collagen gels or Matrigels, they were found to form tubes. In this culture system, co-culture with ECs and/or fibroblasts is not required. It has been suggested that the very malignant cancer stem cell-like melanoma cells with the ability to form tubes express laminin 5 and matrix metalloproteinases 1, 2, and 9 which might be involved in tube formation.

It has been known for some time that tumor cells can form sac-like structures connecting to blood vessels, as shown by their being filled with red blood cells. However, it had not been demonstrated that the tubes generated by tumor cells themselves were actually involved in tumor microcirculation. Therefore, when this concept was published, several questions arose, such as: Are red blood cells to be found in these tubes? Where is the interface between tumor cells and ECs forming these so-called "blood vessels"? What is the biological significance of this tube formation by tumor cells for tumor microcirculation? [12]. Based on electron microscopy, subsequent reports suggested that other tumors can also generate tube-like structures (e.g., ovary and breast cancer) [13]. Researchers who first documented "vasculogenic mimicry" have further analyzed the features of tumor cells constructing tubes more precisely and found that they express vascular endothelial (VE)-cadherin. It is well established that VE-cadherin is specifically expressed in ECs, and is required for the formation of adherent junctions in ECs. Hence, it seems to function to facilitate tube formation in tumor cells [14].

After publication of this work, it was reported that ECs in the tumor environment frequently exhibit chromosomal

abnormalities [15]. Moreover, these were sometimes common between tumor cells and ECs in the same tumor environment [16]. Therefore, it was tempting to conclude that the tumor cells had directly differentiated into ECs, resulting in the hypothesis that CSCs have the ability to give rise to ECs. Thus, "vasculogenic mimicry" leads to a similar concept: that tumor cells themselves adapt to the absence of blood vessels by differentiating into ECs.

Cancer stem cells as source of ECs in tumors

Differentiation of normal tissue-specific stem cell populations into vascular cells such as ECs and mural cells had already been reported for HSCs, as described above [7], as well as for neuronal stem cells [17]. Recently, cancer stem cell isolation has been greatly facilitated by the establishment of CSC markers. Thus, it has been reported that CSCs isolated from a cultured glioblastoma cell line can differentiate into neuronal cells and glial cells [18]. Neuronal stem cells were previously reported to differentiate into ECs. Moreover, it is known that the density of vascularization in glioblastoma is higher than in other tumors. Taken together, these findings support the notion that glioblastoma CSCs can directly differentiate into ECs.

Wang et al. [5] reported that ECs from glioblastoma showed aberrant overexpression of receptors for epidermal growth factor (EGF) as observed in glioblastoma cells themselves. The expression of VE-cadherin and CD133 (a stem cell marker) by tumor cells has been examined and it was concluded that VE-cadherin-positive cells were already committed to ECs regardless of CD133 expression. When candidate CSCs defined as VE-cadherin-negative and CD133-positive were cultured once with cancer cells in vitro and then transferred to collagen gels, they generated tube-like structures and began to express the EC marker CD31. ECs derived from CSCs in this case arose via CD133 and VE-cadherin double-positive cells, possibly EPC (Fig. 3). Interestingly, without prior co-culture with cancer cells, CSCs could not differentiate into ECs. This suggests two possibilities, i.e., cancer-derived factors directly induce differentiation of CSCs into ECs, or an autocrine loop of factors derived from CSCs affected by co-culture with cancer cells is established which induces transdifferentiation of CSCs to ECs.

CD133-positive CSCs have tumor initiation ability but only those from the tumor that are VE-cadherin-negative had the ability to differentiate into ECs. CSCs can produce not only a multitude of cancer cells, resulting in large masses, but may also participate in blood vessel formation as ECs. In terms of anti-tumor angiogenesis blockade, because CSCs originally show drug resistance, those ECs derived from them may also show resistance against

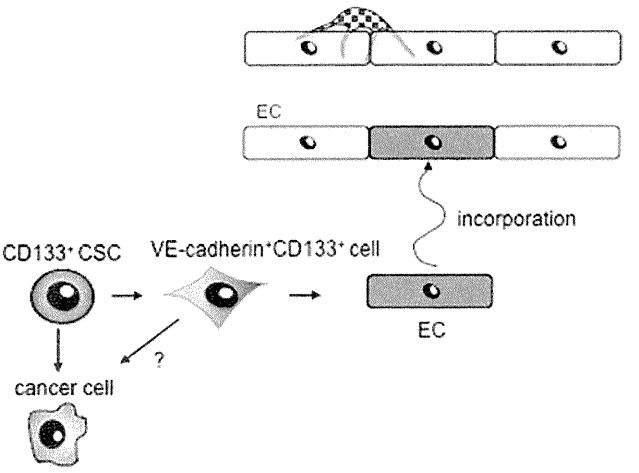

Fig. 3 Differentiation of $CD133^+$ glioblastoma cancer stem cells (CSCs) to ECs through VE-cadherin$^+$CD133$^+$ endothelial progenitor cells. It is not fully understood whether VE-cadherin$^+$CD133$^+$ cells are cancer cells or differentiate into cancer cells

angiogenesis inhibitors. Therefore, it is important to design a strategy for effectively inhibiting the growth of ECs from CSCs. When notch signaling is suppressed in CSCs by γ-secretase inhibitors, differentiation of CD133 and VE-cadherin double-positive endothelial progenitors from CSCs is blocked. Moreover, neutralization of VEGF or suppression of VEGF receptor expression inhibits differentiation of CD133 and VE-cadherin double-positive ECs. Such strategies may contribute to the development of anti-angiogenic therapy targeting the CSC–EC transition.

Along the same lines, Ricci-Vitiani et al. have shown that a comparable proportion of a cell population expressing EC markers and a population of neighboring tumor cells shared a mutated version of the oncogene p53. This also strongly suggested that ECs in the tumor had originated from the cancer cells [6]. Moreover, they found that 30% of ECs express both the EC marker vWF and the glial cell marker GFAP. As also observed by Wang et al., they reported that CD133-positive CSCs could differentiate into ECs both in vitro and in vivo. This work also revealed the biological significance of CSC-derived ECs for tumor growth. A suicide gene, herpes simplex virus thymidine kinase (tk), was transfected into neurosphere-forming CSCs retrovirally and expressed under the transcriptional control of an endothelial-specific gene (Tie2) promoter. In this model, ECs derived from CSCs would be killed by treatment with ganciclovir if it was the CSCs which had differentiated into ECs. It was indeed found that tumor growth was greatly suppressed by the death of CSC-derived ECs. Therefore, it was concluded that ECs derived from CSCs directly contribute to blood vessel formation at least in their model of glioblastoma.

Conclusion

Direct and indirect effects of stem cell populations on blood vessel formation have been reviewed here. In terms of stem cell function in promoting angiogenesis as accessory components indirectly, probably both normal stem cells and CSCs have such an ability in the context of blood vessel formation. However, direct differentiation of CSCs into ECs needs to be verified in cancer histotypes other than glioblastoma, although the possibility of direct differentiation of CD44-positive CSCs into ECs has already been suggested [19].

In the tumor microenvironment, ECs originally play a role in the formation of blood vessels. However, as the stemness of HSCs is supported in the vascular region, the so-called "vascular niche", ECs in the tumor may also act as a niche cell component to support maintenance of stemness of CSCs as well. In terms of stromal cells, it has been suggested that myofibroblasts, cancer-associated fibroblasts, and vascular mural cells all support tumor growth. Recently, it was even reported that ECs can differentiate into mesenchymal stem cells by an endothelial–mesenchymal transition, designated End-MT, when stimulated with TGFβ or BMP2 [8]. Therefore, it is conceivable that ECs derived from CSCs may also differentiate into mesenchymal cells, as above, to support growth of tumor cells. In summary, it is important to understand the molecular mechanisms of EC development from CSCs to develop optimal strategies to inhibit tumor growth.

Acknowledgments This work was supported in part by a grant from the Ministry of Education, Science, Sports, and Culture of Japan.

Conflict of interest The authors declare no competing financial interests.

Refferences

1. Risau W. Mechanisms of angiogenesis. Nature. 1997;386:671–4.
2. Carmeliet P. Angiogenesis in health and disease. Nat Med. 2003;9:653–60.
3. Ferrara N, Kerbel RS. Angiogenesis as a therapeutic target. Nature. 2005;438:967–74.
4. Jain RK. Normalization of tumor vasculature: an emerging concept in antiangiogenic therapy. Science. 2005;307:58–62.
5. Wang R, Chadalavada K, Wilshire J, Kowalik U, Hovinga KE, Geber A, et al. Glioblastoma stem-like cells give rise to tumour endothelium. Nature. 2010;468:829–33.
6. Ricci-Vitiani L, Pallini R, Biffoni M, Todaro M, Invernici G, Cenci T, et al. Tumour vascularization via endothelial differentiation of glioblastoma stem-like cells. Nature. 2010;468:824–8.
7. Yamada Y, Takakura N. Physiological pathway of differentiation of hematopoietic stem cell population into mural cells. J Exp Med. 2006;203:1055–65.
8. Medici D, Shore EM, Lounev VY, Kaplan FS, Kalluri R, Olsen BR. Conversion of vascular endothelial cells into multipotent stem-like cells. Nat Med. 2010;16:1400–6.
9. Crisan M, Yap S, Casteilla L, Chen C, Corselli M, Park TS, et al. A perivascular origin for mesenchymal stem cells in multiple human organs. Cell Stem Cell. 2008;3:301–13.
10. Takakura N, Watanabe T, Suenobu S, Yamada Y, Noda T, Ito Y, et al. A role for hematopoietic stem cells in promoting angiogenesis. Cell. 2000;102:199–209.
11. Maniotis AJ, Folberg R, Hess A, Seftor EA, Gardner LM, Pe'er J, et al. Vascular channel formation by human melanoma cells in vivo and in vitro: vasculogenic mimicry. Am J Pathol. 1999;155:739–52.
12. McDonald DM, Munn L, Jain RK. Vasculogenic mimicry: how convincing, how novel, and how significant? Am J Pathol. 2000;156:383–8.
13. Hendrix MJ, Seftor EA, Hess AR, Seftor RE. Vasculogenic mimicry and tumour-cell plasticity: lessons from melanoma. Nat Rev Cancer. 2003;3:411–21.
14. Hendrix MJ, Seftor EA, Meltzer PS, Gardner LM, Hess AR, Kirschmann DA, et al. Expression and functional significance of VE-cadherin in aggressive human melanoma cells: role in vasculogenic mimicry. Proc Natl Acad Sci USA. 2001;98:8018–23.
15. Hida K, Hida Y, Amin DN, Flint AF, Panigrahy D, Morton CC, et al. Tumor-associated endothelial cells with cytogenetic abnormalities. Cancer Res. 2004;64:8249–55.
16. Streubel B, Chott A, Huber D, Exner M, Jäger U, Wagner O, et al. Lymphoma-specific genetic aberrations in microvascular endothelial cells in B-cell lymphomas. N Engl J Med. 2004;351:250–9.
17. Wurmser AE, Nakashima K, Summers RG, Toni N, D'Amour KA, Lie DC, et al. Cell fusion-independent differentiation of neural stem cells to the endothelial lineage. Nature. 2004;430:350–6.
18. Kondo T, Setoguchi T, Taga T. Persistence of a small subpopulation of cancer stem-like cells in the C6 glioma cell line. Proc Natl Acad Sci USA. 2004;101:781–6.
19. Alvero AB, Chen R, Fu HH, Montagna M, Schwartz PE, Rutherford T, et al. Molecular phenotyping of human ovarian cancer stem cells unravels the mechanisms for repair and chemoresistance. Cell Cycle. 2009;8:158–66.

Int J Hematol (2012) 95:117–118
DOI 10.1007/s12185-012-1014-0

Guest editorial: mutual relationship between vascular biology and hematology

Nobuyuki Takakura

Received: 18 January 2012 / Revised: 19 January 2012 / Accepted: 19 January 2012 / Published online: 7 February 2012

Vascular biology has rapidly progressed in a molecular level since the identification of growth factors regulating blood vessel formation in the mid-1990s. In contrast to hematology, in which cytokines involved in the development and proliferation of hematopoietic cells (HCs) were first identified and analyzed in the 1980s, vascular biology has a short history, as analysis of the mechanisms underlying blood vessel formation were started at the molecular level. Inhibitors of vascular endothelial growth factors (VEGFs) or their cognate receptors have, however, already entered clinical use in the treatment of cancer and retinopathy. Moreover, therapeutic angiogenesis by such methods as gene transfer, bone marrow cell injection, and cytokine administration has also entered clinical use. It is no exaggeration to say that translation from bench to bed side has proceeded extremely rapidly in vascular biology.

Recognition of the intimate interaction between hematopoiesis and blood vessel formation emerged from histological analyses showing that hematopoietic cells and vascular endothelial cells (ECs) originate from a common ancestor, known as the hemangioblast. However, several lines of evidence suggest that hematopoietic cells are derived from cells which have already committed to ECs, so-called hemogenic angioblasts, during embryogenesis. In the adult, however, bone marrow hematopoietic cells can differentiate into vascular cells, such as ECs and vascular smooth muscle-like cells. Clearly, these two populations follow complex developmental routes. Moreover, functionally, hematopoietic cells support angiogenesis as an accessory cell component, and, conversely, blood vessels provide a niche for the maintenance of the stemness of hematopoietic stem cells.

Clinically, bone marrow hematopoietic cell infusion therapy to induce angiogenesis for ischemic diseases, such as chronic lower extremity occlusive disease or ischemic heart disease, is one example of the utilization of the intimate interaction between hematopoiesis and vascular development. Usage of the hematopoiesis-related cytokine, G-CSF, in the mobilization of bone marrow hematopoietic stem/progenitor cells into peripheral blood to facilitate the recruitment of such cells to ischemic regions is one example of a strategy that brings together the fields of hematology and vascular biology.

In this PIH review series, a number of research approaches linking hematopoiesis and vascular biology are introduced. Dr. Beate Heissig overviews the mechanism of fibrinolysis for bone marrow cell mobilization associated with induction of angiogenesis, while Dr. Hideto Matsui discusses a strategy for the treatment of congenital coagulation defects using gene transfer into bone marrow endothelial progenitors. It is widely accepted that suppression of angiogenesis is a promising method for inhibiting tumor growth. By contrast, Dr. Yusuke Mizukami argues that induction of angiogenesis in tumor may also represent an effective alternative for tumor growth inhibition, as a means of providing routes of drug delivery. He introduces new blood vessel formation in tumor using bone marrow cells. Finally, the function of hematopoietic stem cells in the promotion of angiogenesis is reviewed, along with recent topics pointing to angiogenesis-related functions in cancer stem cells. The function of stem cells in promoting blood vessel formation may be closely associated with the formation of the vascular niche for stem cell maintenance, and, therefore, stem cells themselves may construct the foci needed to maintain their own stemness.

N. Takakura (✉)
Research Institute for Microbial Diseases,
Osaka University, Suita, Osaka 565-0871, Japan
e-mail: ntakaku@biken.osaka-u.ac.jp

It will be important to gain a better understanding of the precise molecular mechanisms behind blood vessel formation by stem cells, and to determine the vascular niche component if we are to develop effective strategies in both regeneration and cancer therapy.

Compared with research in hematology, in which extensive molecular analyses of lineage commitment from hematopoietic stem cells to well-differentiated mature hematopoietic cells have been performed, lineage analysis of the differentiation of vascular stem cells to mature ECs is yet to be addressed in vascular biology. While hematopoietic stem cells can be identified using a profile of surface molecules and isolated to analyze their differentiation, there are still no molecular markers of endothelial stem cells, and indeed, the endothelial stem cell itself has not been definitively identified. It is still unclear whether endothelial stem cells are present in the adult; however, as there are three different types of ECs during angiogenesis, they may still await identification. Tip cells are sprouted from pre-existing blood vessel in the initiation of angiogenesis and located in front of new vascular branch; however, these lack proliferative ability. Stalk cells situated behind the tip cells proliferate and induce the elongation of new branches. Finally, phalanx cells emerge, stabilize and mature into newly developed blood vessels. This heterogeneity of ECs suggests that there may be endothelial stem cells that produce different types of ECs. Vascular biology may grow even further once endothelial stem cells have been defined, and therapy for vascular diseases, including the suppression and induction of blood vessel formation, is improved.

Published OnlineFirst on May 6, 2011; DOI:10.1158/1535-7163.MCT-10-0707

Molecular Cancer Therapeutics

E7080 Suppresses Hematogenous Multiple Organ Metastases of Lung Cancer Cells with Nonmutated Epidermal Growth Factor Receptor

Hirokazu Ogino, Masaki Hanibuchi, Soji Kakiuchi, et al.

Mol Cancer Ther Published OnlineFirst May 6, 2011.

Published OnlineFirst on May 6, 2011; DOI:10.1158/1535-7163.MCT-10-0707

Preclinical Development

Molecular Cancer Therapeutics

E7080 Suppresses Hematogenous Multiple Organ Metastases of Lung Cancer Cells with Nonmutated Epidermal Growth Factor Receptor

Hirokazu Ogino[1], Masaki Hanibuchi[1], Soji Kakiuchi[1,2], Van The Trung[1], Hisatsugu Goto[1], Kenji Ikuta[1], Tadaaki Yamada[1,4], Hisanori Uehara[3], Akihiko Tsuruoka[5], Toshimitsu Uenaka[5], Wei Wang[4], Qi Li[4], Shinji Takeuchi[4], Seiji Yano[4], Yasuhiko Nishioka[1], and Saburo Sone[1,2]

Abstract

While epidermal growth factor receptor (EGFR) tyrosine kinase inhibitors improve the prognosis of patients with *EGFR* mutant lung cancer, the prognosis of patients with nonmutant *EGFR* lung cancer, especially those with metastases, is still extremely poor. We have assessed the therapeutic efficacy of E7080, an orally available inhibitor of multiple tyrosine kinases including VEGF receptor 2 (VEGFR-2) and VEGFR-3, in experimental multiple organ metastasis of lung cancer cell lines without *EGFR* mutations. E7080 markedly inhibited the *in vitro* proliferation of VEGF-stimulated microvascular endothelial cells. Intravenous inoculation into natural killer cell–depleted severe combined immunodeficient mice of the small cell lung cancer cell lines H1048 (producing low amounts of VEGF) and SBC-5 (producing intermediate amounts of VEGF) resulted in hematogenous metastases into multiple organs, including the liver, lungs, kidneys, and bones, whereas intravenous inoculation of PC14PE6, a non–small cell lung cancer cell line producing high amounts of VEGF, resulted in lung metastases followed by massive pleural effusion. Daily treatment with E7080 started after the establishment of micrometastases significantly reduced the number of large (>2 mm) metastatic nodules and the amount of pleural effusion, and prolonged mouse survival. Histologically, E7080 treatment reduced the numbers of endothelial and lymph endothelial cells and proliferating tumor cells and increased the number of apoptotic cells in metastatic nodules. These results suggest that E7080 has antiangiogenic and antilymphangiogenic activity and may be of potential therapeutic value in patients with nonmutant *EGFR* lung cancer and multiple organ metastases. *Mol Cancer Ther; 10(7); 1–11.* ©*2011 AACR.*

Introduction

Lung cancer is one of the most prevalent malignancies and the leading cause of cancer-related deaths worldwide (1). The high mortality of this disease is predominantly due to the high metastatic potential of lung cancer. Although platinum-based cytotoxic chemotherapy is standard treatment for both small cell lung cancer (SCLC) and non–small cell lung cancer (NSCLC) with metastases (2), the median survival of these patients is only about 12 to 14 months. Recently, epidermal growth factor receptor (EGFR) tyrosine kinase inhibitors have been shown to prolong progression-free survival of lung cancer patients with tumors containing mutated *EGFR*, extending the median survival of these patients to 22 to 30 months (3, 4). Nevertheless, the prognosis of patients with metastatic SCLC and NSCLC with nonmutant *EGFR* lung cancer has not yet been improved (5).

Angiogenesis is essential for tumor enlargement and metastasis and is regulated by proangiogenic and antiangiogenic molecules (6). VEGF-related molecules (VEGF, VEGF-B, VEGF-C, VEGF-D, and placental growth factor) and receptors (VEGFR-1, VEGFR-2, and VEGFR-3) play pivotal roles in angiogenesis and lymphangiogenesis (7). Binding of VEGF to VEGFR-2 is the critical signal for tumor angiogenesis, as well as inducing vascular hyperpermeability and promoting the production of pleural effusion and ascites (8, 9). VEGF-C and VEGF-D activate VEGFR-3 and are considered lymphangiogenic factors, although the fully processed form of VEGF-C also

Authors' Affiliations: Departments of [1]Respiratory Medicine and Rheumatology, [2]Medical Oncology, and [3]Molecular and Environmental Pathology, Institute of Health Biosciences, University of Tokushima Graduate School, Tokushima; [4]Division of Medical Oncology, Cancer Research Institute, Kanazawa University, Ishikawa; and [5]Discovery Department, Oncology PCU, Eisai Product Creation Systems, Research Laboratories, Eisai Co. Ltd., Ibaraki, Japan

Note: Supplementary material for this article is available at Molecular Cancer Therapeutics Online (http://mct.aacrjournals.org/).

Corresponding Author: Saburo Sone, Department of Respiratory Medicine and Rheumatology, Institute of Health Biosciences, University of Tokushima Graduate School, 3-18-15 Kuramoto-cho, Tokushima 770-8503, Japan. Phone: 81-88-633-7127; Fax: 81-88-633-2134; E-mail: ssone@clin.med.tokushima-u.ac.jp

doi: 10.1158/1535-7163.MCT-10-0707

Published OnlineFirst on May 6, 2011; DOI:10.1158/1535-7163.MCT-10-0707

activates VEGFR-2 (10). In addition, the binding of VEGF-C to VEGFR-3 has been found to promote intratumoral lymphangiogenesis and lymph node metastasis in a preclinical study (11).

The anti-VEGF monoclonal antibody, bevacizumab, has been used successfully to treat patients with several malignant diseases including nonsquamous NSCLC (12, 13). However, the combination of bevacizumab and cytotoxic chemotherapy has been found to have marginal effects on patient survival (12, 14), suggesting the need for novel therapeutic modalities.

E7080 is an orally active inhibitor of VEGFR-2 and VEGFR-3, with additional activity against other receptor tyrosine kinases, including fibroblast growth factor receptors (FGFR), platelet-derived growth factor receptors (PDGFR), and c-Kit (15). E7080 shows potent antitumor effects in xenograft models of various types of tumors by inhibiting angiogenesis, especially through VEGFR-2/3 suppression (16, 17). We have tested the therapeutic efficacy of E7080 against lung cancer cell lines expressing wild-type EGFR, using *in vivo* experimental metastasis models.

Materials and Methods

Cell lines

The human SCLC cell line SBC-5 and a human NSCLC cell line PC14PE6 were kindly provided by Drs. M. Tanimoto and K. Kiura (Okayama University, Okayama, Japan; ref. 18) in 2006 and Dr. I. J. Fidler (M.D. Anderson Cancer Center, Houston, TX; ref. 9) in 1999, respectively. The human SCLC cell line H1048 and human NSCLC cell line PC-9 were purchased from American Type Culture Collection in 2004 and Immuno-Biological Laboratories Co.; ref. 19) in 2007, respectively. Flow cytometric analyses revealed that H1048, PC14PE6, and SBC-5 cells showed high, intermediate, and very low wild-type EGFR protein expression, respectively (data not shown). SBC-5 cells were maintained in Eagle's Minimum Essential Media (MEM) and H1048, PC14PE6, and PC-9 cells were maintained in RPMI 1640 medium, each supplemented with 10% heat-inactivated FBS, penicillin (100 U/mL), and streptomycin (50 μg/mL). Human dermal microvascular endothelial cells (HMVEC) were purchased from KURABO in 2007 and maintained in HuMedia-MvG with growth supplements (KURABO). All cells were passaged for less than 3 months before renewal from frozen, early-passage stocks obtained from the indicated sources. Cells were regularly screened for *Mycoplasma* with the use of a MycoAlert Mycoplasma Detection Kit (Lonza). All cells were cultured at 37°C in a humidified atmosphere of 5% CO_2 in air.

Reagents

4-[3-Chloro-4-(*N*′-cyclopropylureido)phenoxy]-7-methoxyquinoline-6-carboxamide (E7080) was synthesized by Eisai Co. Ltd., as described (15, 16). For *in vitro* experiments, a stock solution of E7080 (10 mmol/L) was prepared in dimethyl sulfoxide, stored at −20°C, and diluted with culture media before use. For *in vivo* experiments, E7080 was dissolved in distilled water and stored until use at 4°C. Recombinant human VEGF165 and recombinant human basic fibroblast growth factor (bFGF) were purchased from R&D Systems. An anti-mouse interleukin 2 receptor β-chain monoclonal antibody, TM-β1 (IgG2b), was supplied by Drs. M. Miyasaka and T. Tanaka (Osaka University, Osaka, Japan; ref. 20).

Expression of VEGF, VEGF-C, VEGF-D, and VEGFR mRNAs

Expression of VEGF, VEGF-C, VEGF-D, and VEGFR mRNAs was measured by reverse transcriptase (RT) PCR. Total cellular RNA was isolated using RNeasy Mini kits and RNase-free DNase kits (Qiagen) according to the manufacturer's protocols. Total RNAs were reversely transcribed using an Omniscript RT kit (Qiagen). PCRs were carried out using Ex Taq Hot Start Version (Takara) and the primers are shown in Supplementary Table S1. RT-PCR products were electrophoresed on agarose gels, and the bands were visualized by ethidium bromide staining.

VEGF production

Tumor cells (1×10^6) were cultured in RPMI 1640 medium with 10% FBS for 24 hours. The cells were washed with PBS and incubated for 48 hours in RPMI 1640 medium with 10% FBS. The culture medium was harvested and centrifuged, and the supernatants were stored at −70°C until analysis. VEGF concentration was assayed by ELISA as described by the manufacturer (R&D Systems). All samples were run in triplicate, and each assay was conducted 3 times independently.

Flow cytometric analysis

HMVECs and tumor cells were harvested and resuspended in PBS. After 2 washes with PBS, the cells were incubated for 45 minutes at 4°C with phycoerythrin (PE)-labeled anti VEGFR-1, VEGFR-2, and VEGFR-3 antibodies or with PE-labeled mouse IgG1 antibody. The intensity of fluorescence was measured by flow cytometric analysis using FACScan (Becton Dickinson).

Cell proliferation assay

Cell proliferation was measured using the MTT dye reduction method (21). Briefly, tumor cells (2×10^3 cells per 100 μL per well), plated in triplicate in 96-well plates, were incubated in medium containing 10% FBS for 24 hours. HMVECs (5×10^3 cells per 100 μL per well), plated in triplicate in 96-well plates precoated with 1.5% gelatin, were incubated in Eagle's MEM containing 5% FBS for 24 hours. Tumor cells were incubated with several concentrations of E7080 for a further 72 hours. HMVECs were incubated for 72 hours with E7080 in the presence or absence of VEGF or bFGF. To each well was added 50 μL of MTT solution (2 mg/mL; Sigma), followed by incubation for a further 2 hours. The media containing

Published OnlineFirst on May 6, 2011; DOI:10.1158/1535-7163.MCT-10-0707

MTT solution were removed, and the dark blue crystals in each well were dissolved in 100 μL dimethyl sulfoxide. The absorbance was measured at test and reference wavelengths of 550 and 630 nm, respectively.

To determine the bioactivity of VEGF produced by the tumor cells, WST assays were conducted using Cell Counting Kit-8 (Dojindo). Briefly, HMVECs (5×10^3 cells per 100 μL per well) were plated in triplicate in 96-well plates precoated with 1.5% gelatin. After 24 hours, HMVECs were incubated with cell culture supernatants of tumor cells in the presence or absence of E7080 (10 nmol/L) for 72 hours. Following the addition of 10 μL of WST-8 reagents, the cells were incubated for a further 2 hours, and absorbance was measured at 450 nm and 630 nm.

Western blot analysis

HMVECs were cultured until confluence in EBM medium containing 0.5% FBS for 24 hours. Cells were treated with E7080 at indicated concentrations for 120 minutes, stimulated with VEGF165 (20 ng/mL) for 10 minutes, and collected in Cell Lysis Buffer (Cell Signaling Technology) containing 1 mmol/L phenylmethylsulfonylfluoride. Protein concentrations were determined using a BCA protein assay kit (Pierce Biotechnology). For Western blot analysis, 20 μg of total protein was resolved by SDS-PAGE (Bio-Rad) and transferred to polyvinylidene difluoride membranes (Atto). After 3 washes, the membranes were incubated with Blocking One (Nacalai Tesque Inc.) for 1 hour at room temperature and incubated overnight at 4°C with 1:1,000 dilutions of primary antibodies to p-VEGFR-2 (Tyr 996; Cell Signaling Technology), VEGFR-2 (C-1158; Santa Cruz Biotechnology), phospho-p44/p42 MAPK (Thr202/Tyr204; Cell Signaling Technology), and p44/p42 MAPK (Cell Signaling Technology). After washing, the membranes were incubated for 2 hours at room temperature with species-specific horseradish peroxidase–conjugated secondary antibodies. Immunoreactive bands were visualized using enhanced chemiluminescent substrate (Pierce Biotechnology).

Animals

Male severe combined immunodeficient mice (SCID) mice and athymic BALB/c nude mice, 5 to 6 weeks old, were obtained from CLEA Japan and maintained under specific pathogen-free conditions throughout this study. All experiments were carried out in accordance with the guidelines established by the Tokushima University Committee on Animal Care and Use.

In vivo metastasis models

To facilitate metastasis formation, SCID mice were pretreated with anti-mouse interleukin 2 receptor β-chain antibody to deplete natural killer (NK) cells (20). Two days later, the mice were inoculated with SBC-5 or H1048 cells (1.0×10^6 per mouse) into the tail vein. Nude mice were intravenously inoculated via the tail vein with PC14PE6 cells (1.0×10^6 per mouse). As we reported previously, micrometastases were detected as early as 14 days after tumor cell inoculation (9). To evaluate the therapeutic efficacy of E7080 against established metastatic nodules, the mice were treated once daily with 1, 3, and 10 mg/kg/d E7080 by oral gavage, beginning 2 (SBC-5 and PC14PE6 cells) or 4 weeks (H1048 cells) after inoculation. Five (SBC-5 and PC14PE6 cells) or 8 weeks (H1048 cells) after tumor cell inoculation, the mice were anesthetized by intraperitoneal injection of pentobarbital, and radiographs were taken to determine bone metastases. The mice were killed humanely under anesthesia and the major organs were removed and weighed. The lungs were fixed in Bouin's solution (Sigma) for 24 hours. The number of metastatic colonies on the surface of the organs and the number of osteolytic lesions evident in radiograms were counted by 2 investigators independently (H. Ogino and M. Hanibuchi). To determine the effect of E7080 on survival, mice (10 per group) were treated once daily with 10 mg/kg/d E7080 from day 14 until they became moribund.

Immunohistochemical-immunofluorescent determination of endothelial cells, proliferating and apoptotic tumor cells, and VEGF production

Major organs containing metastases were fixed in 10% formalin and embedded in paraffin, or TissueTek optimum cutting temperature medium (Sakura) and frozen immediately. The paraffin-embedded tissues were used to quantitate *in vivo* cell proliferation using mouse anti-human Ki-67 mAb (MIBI; 1:50 dilution; DAKO), apoptosis using the terminal deoxyribonucleotidyl transferase–mediated dUTP nick end labeling (TUNEL) method with the Apoptosis Detection System (Promega), and VEGF production using mouse anti-human VEGF mAb (1:100 dilution; Pharmingen). To detect endothelial cells, frozen tissue sections (10 μm thick) were fixed with cold acetone and incubated with rat anti-mouse CD31/PECAM-1 monoclonal antibody (1:100 dilution; Pharmingen). To detect lymph endothelial cells, frozen sections were fixed with midl form and incubated with rabbit anti-mouse LYVE-1 monoclonal antibody (1:100 dilution; Abcam). Appropriate secondary antibodies conjugated with peroxidase and the 3,3′-diaminobenzidine tetrahydrochloride (DAB) Liquid System (DakoCytomation) was used to detect immunostaining. To detect CD31 and LYVE-1 simultaneously, frozen sections were fixed with midl form for 1 minute and incubated with rat anti-mouse CD31 and rabbit anti-mouse LYVE-1 antibodies, followed by incubation with anti-rat IgG conjugated to Alexa488 (green) and anti-rabbit IgG conjugated to Alexa594 (red; 1:100 dilution; Molecular Probes). In each analysis, the 5 areas containing the highest number of stained cells within a section were selected for histologic quantification under light microscopy or fluorescent microscopy with a 200-fold magnification. The results were independently evaluated by 2 investigators (H. Ogino and M. Hanibuchi).

Published OnlineFirst on May 6, 2011; DOI:10.1158/1535-7163.MCT-10-0707

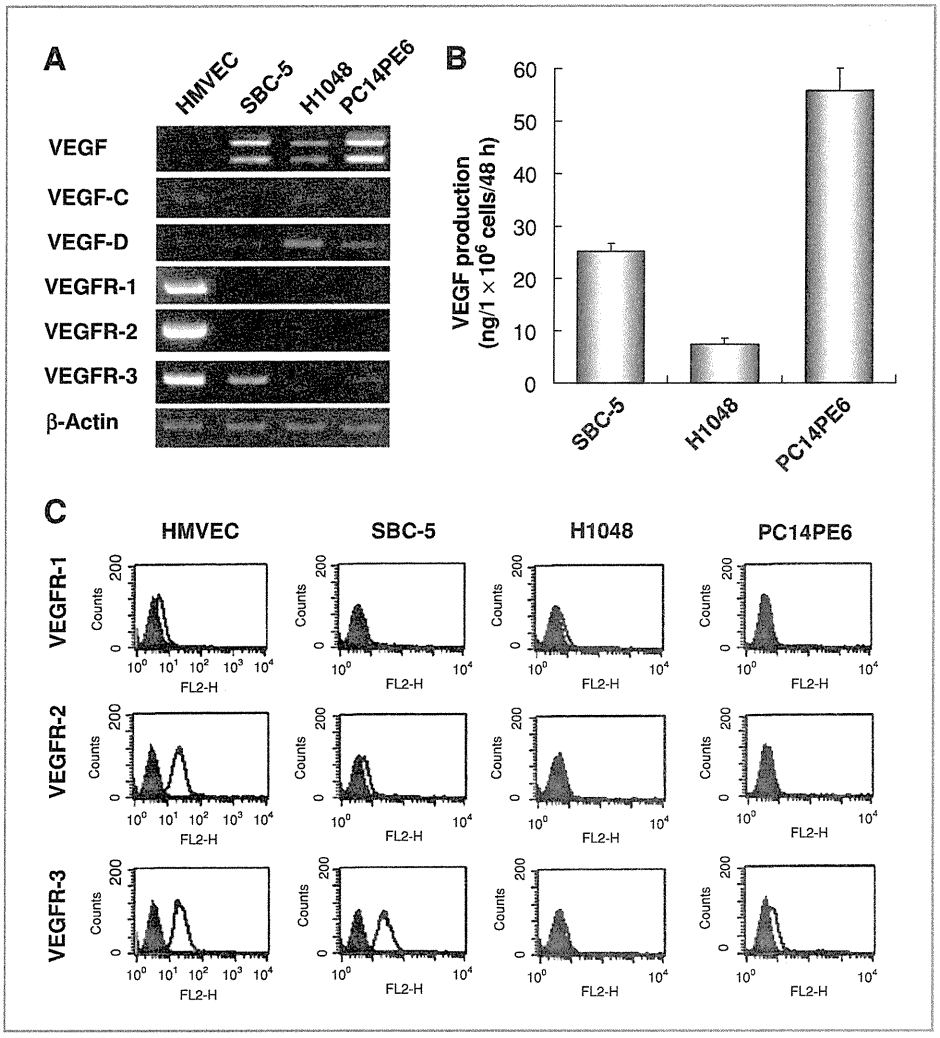

Figure 1. *In vitro* production of VEGF by lung cancer cell lines bearing nonmutant EGFR. A, expression of mRNAs encoding members of the VEGF and VEGFR families in human lung cancer cell lines and endothelial cells (HMVEC) bearing nonmutant EGFR as determined by RT-PCR. B, VEGF production by lung cancer cells bearing nonmutant EGFR as determined by ELISA. C, expression of VEGFRs protein by HMVECs and lung cancer cell lines bearing nonmutant EGFR as determined by flow cytometry.

Statistical analysis

Differences were analyzed by 1-way ANOVA, followed when appropriate by Newman–Keuls multiple comparison tests. Values of $P < 0.05$ were considered statistically significant. All statistical analyses were conducted using the GraphPad Prism Program Ver. 4.01.

Results

Expression of VEGF, VEGF-C, VEGF-D, and their receptors in human endothelial cells and lung cancer cell lines *in vitro*

We determined the expression of VEGF, VEGF-C, VEGF-D, and their receptors in HMVECs and 3 lung cancer cell lines at both the mRNA and protein levels. PC14PE6, SBC-5, and H1048 cells showed high, intermediate, and low VEGF expression, respectively (Fig. 1A and B). Although VEGFR-1 and VEGFR-2 were expressed only in HMVECs, both SBC-5 cells and HMVECs expressed VEGFR-3 mRNA and protein (Fig. 1A and C). However, we could not detect the production of its ligands, VEGF-C and VEGF-D, in the 3 lung cancer cell lines by ELISA (data not shown). Although these cell lines expressed mRNA of several receptors, including FGFR-1, FGFR-2, PDGFR-α, PDGFR-β, and c-kit, the level was generally very low (Supplementary Fig. S1). We also examined the production of ligands for FGFRs (acidic FGF and bFGF), PDGFRs (PDGF-AA, PDGF-AB, and PDGF-BB), and c-Kit (stem cell factor). The levels of these ligands were much lower than that of VEGF (data not shown).

E7080 inhibition of VEGF-induced proliferation and VEGFR-2 phosphorylation of endothelial cells, but not tumor cells, *in vitro*

Chemical structure of E7080 was shown in Fig. 2A. When we assayed the effect of the multiple tyrosine kinase inhibitor, E7080, on the proliferation of tumor cells and endothelial cells *in vitro*, we found that E7080 did not inhibit the proliferation of the 3 human lung cancer cells ($IC_{50} > 1{,}000$ nmol/L; Fig. 2B). In contrast, low-dose E7080 suppressed the proliferation of VEGF-stimulated HMVECs

Published OnlineFirst on May 6, 2011; DOI:10.1158/1535-7163.MCT-10-0707

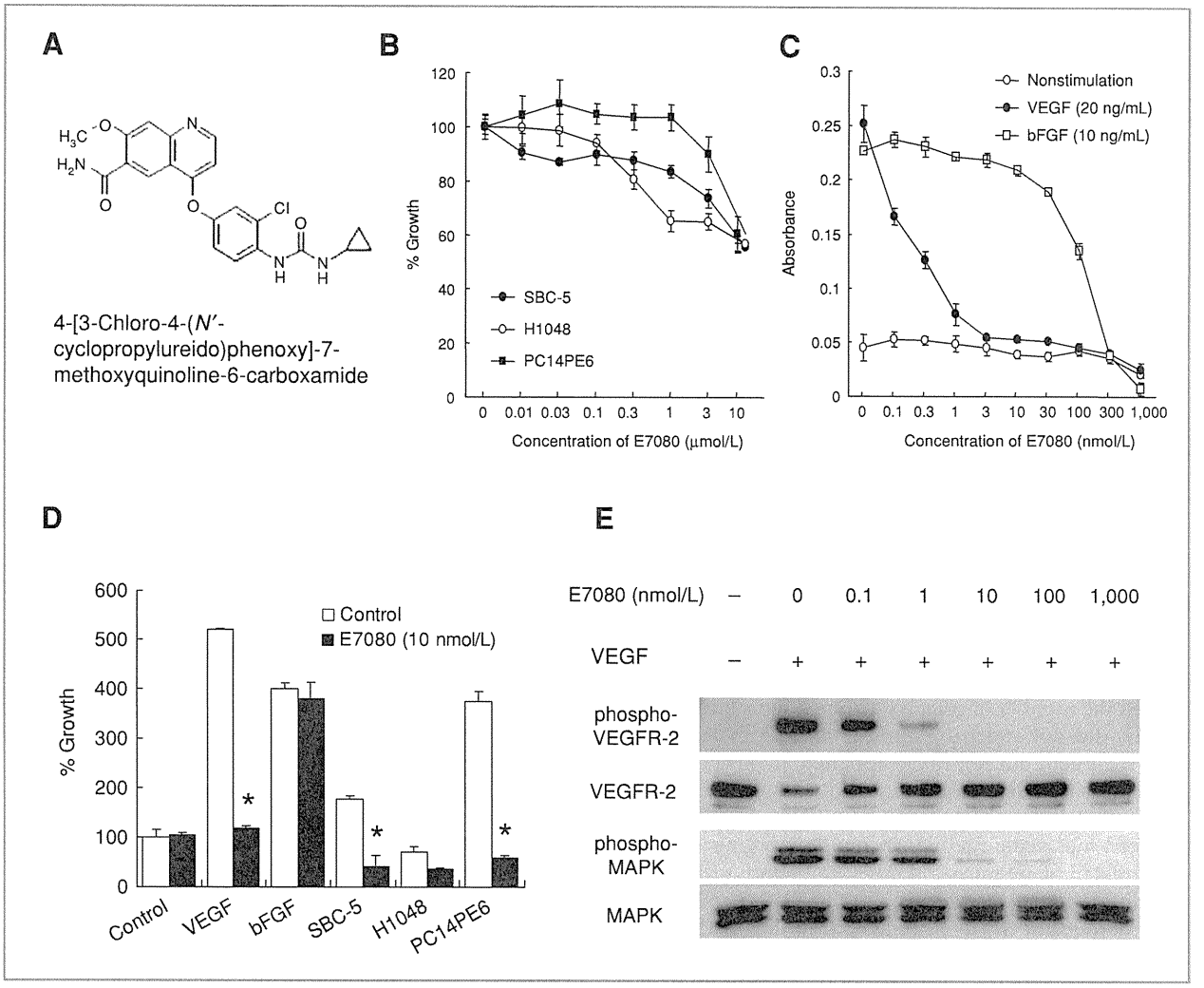

Figure 2. E7080 inhibition of VEGF-induced endothelial proliferation via inhibition of VEGFR-2 phosphorylation. A, chemical structure of E7080. B–D, effect of E7080 on the proliferation of lung cancer cell lines bearing nonmutant EGFR (B), human endothelial cells (HMVEC) stimulated with recombinant VEGF and bFGF (C), and HMVECs stimulated with culture medium from lung cancer cell lines bearing nonmutant EGFR (D) as determined by MTT assays. E, effect of E7080 on VEGFR-2 phosphorylation as determined by Western blot analysis.

(IC_{50} = 0.3 nmol/L), whereas high-dose E7080 suppressed the proliferation of bFGF-stimulated HMVECs (IC_{50} = 100 nmol/L; Fig. 2C). The culture supernatants of SBC-5 and PC14PE6 cells stimulated HMVEC proliferation, effects abrogated by 10 nmol/L E7080, a dose sufficient to inhibit the proliferation of HMVECs induced by VEGF but not by bFGF (Fig. 2D). These results suggest that VEGF but not bFGF may be the predominant tumor cell–derived growth factor for HMVEC produced by these lung cancer cell lines.

E7080 also dose dependently suppressed the VEGF-induced VEGFR-2 phosphorylation and activation of downstream signaling pathways, such as the mitogen-activated protein kinase (MAPK) pathway, in HMVECs (Fig. 2E), suggesting that E7080 has potent activity against VEGF-induced angiogenesis. We also confirmed that E7080 inhibited VEGF-C–induced phosphorylation of VEGFR-3 (Supplementary Fig. S2), in agreement with previous results (16).

E7080 suppression of enlargement of metastases of lung cancer cells expressing nonmutant EGFR in immunodeficient mice

We next examined the effect of E7080 on metastasis induced by lung cancer cells expressing nonmutant *EGFR*. Intravenous inoculation of the SCLC cell line, SBC-5, into NK cell–depleted SCID mice has been shown to produce experimental metastases within 35 days (22–24). These metastatic lesions were located primarily in the liver where some were greater than 2 mm in diameter. In addition, SBC-5 cells produce lung metastases (<2 mm in diameter) and osteolytic bone metastases detectable by radiography (Fig. 3 and Table 1). Treatment with E7080

Published OnlineFirst on May 6, 2011; DOI:10.1158/1535-7163.MCT-10-0707

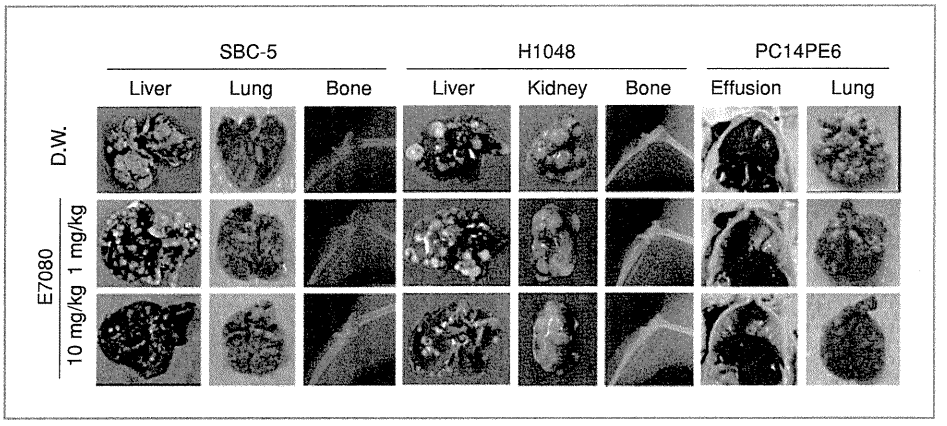

Figure 3. E7080 inhibition of the enlargement of hematogenous multiple organ metastases of lung cancer cells bearing nonmutant *EGFR* in immunodeficient mice. SBC-5 and H1048 cells were inoculated intravenously into NK cell–depleted SCID mice, whereas PC14PE6 cells were intravenously inoculated into nude mice. Mice received oral E7080 on days 14 to 35 after inoculation with SBC-5 or PC14PE6 cells and on days 28 to 56 after inoculation with H1048 cells. Representative pictures of 5 to 8 mice per group are shown. D.W., distilled water.

reduced significantly the number of large liver metastases (>2 mm in diameter) and total liver weight even at low doses (1 mg/kg/d) but did not reduce the total number of liver metastases (Fig. 3 and Table 1). At higher doses (3 and 10 mg/kg/d), E7080 also significantly reduced the number of osteolytic bone lesions but, interestingly, did not affect the number of lung metastases. E7080 treatment did not cause apparent adverse events, such as loss of body weight (data not shown).

We found that a second SCLC cell line, H1048, also produced metastatic nodules in multiple organs of NK cell–depleted SCID mice, although its pattern of metastases differed from that of SBC-5 cells. H1048 cells produced nodules in the liver, kidneys, and bones (Fig. 3). Once daily treatment with high dose (10 mg/kg/d), but not low dose (1 mg/kg/d), E7080 suppressed the number of large metastases in the liver and kidneys, as well as reducing the total weight of the liver and kidney and the number of metastatic nodules in bone (Fig. 3 and Table 1).

In contrast, human lung adenocarcinoma cells, PC14PE6, produced large colonies only in the lung and induced large volumes of pleural effusion in nude mice (Fig. 3 and Table 1; refs. 9, 25). Treatment with E7080 reduced significantly the number of large lung metastases and total lung weight even at low doses (1 mg/kg/d), as well as completely suppressing the production of pleural effusion (Fig. 3 and Table 1). These results suggest that E7080 may prevent the enlargement of metastatic colonies in multiple organs including the lungs.

E7080 inhibition of the growth of macroscopically detectable metastatic nodules

We previously reported that intravenously inoculated SBC-5 cells produce micrometastases and macroscopically detectable metastatic nodules within 14 and 21 days, respectively (22). We therefore determined whether treatment with E7080 could inhibit the growth of macroscopically detectable metastases. Treatment of E7080, started on day 14 or 21, inhibited the numbers of bone and liver metastases larger than 2 mm in diameter (Supplementary Table S2), indicating that E7080 has therapeutic activity against not only micrometastases but macroscopically detectable metastases.

E7080 inhibition of angiogenesis and lymphangiogenesis in metastatic nodules

Histologic analysis showed that treatment with E7080 caused necrosis in liver metastases produced by SBC-5 cells (Fig. 4A). Because E7080 has activity against VEGFR-2 and VEGFR-3, which are crucial for angiogenesis and lymphangiogenesis, we evaluated the effects of E7080 on angiogenesis and lymphangiogenesis, as well as on proliferating and apoptotic cells in the metastases. CD31-positive cells, presumably representing endothelial cells, were detected diffusely in metastatic nodules, whereas LYVE-1–positive cells, presumably representing lymph endothelial cells, were detected predominantly in the periphery of the nodules (Fig. 4A). Double staining for CD31 and LYVE-1 showed that a small population of cells in the periphery was doubly positive for both (Fig. 4B), consistent with previous findings (26, 27). Importantly, E7080 treatment dramatically inhibited the numbers of CD31- and LYVE-1–positive cells (Fig. 4A and C). Moreover, E7080 treatment decreased the number of Ki-67–positive proliferating tumor cells and increased the number of TUNEL-positive apoptotic cells in liver metastases (Fig. 4A and C). There was no discernible difference in VEGF production between control and E7080-treated tumors (Supplementary Fig. S3). These results indicate that E7080 can inhibit both angiogenesis and lymphangiogenesis and therefore suppress the growth of metastases.

E7080 prolongation of the survival of mice bearing metastases of nonmutant EGFR lung cancer cells

We finally determined whether E7080 could prolong the survival of mice bearing metastases. SBC-5 and

Table 1. Therapeutic effect of oral treatment with E7080 on the multiple organ metastasis produced by non-EGFR mutant lung cancer cell lines in immunodeficient mice

Cell line	Treatment	Liver			Lung			Kidney			Bone
		Weight, g	No. of metastasis		Weight, mg	No. of metastasis		Weight, mg	No. of metastasis		No. of metastasis
			All nodules	>2 mm[a]		All nodules	>2 mm		All nodules	2 mm	
SBC-5 ($N = 5$)	Control	2.0 (1.1–2.7)[b]	89 (58–95)	64 (35–73)	195 (162–212)	66 (46–101)	All 0	N/A			11 (8–11)
	E7080										
	1 mg/kg	1.1 (0.9–1.4)[c]	59 (29–78)	30 (14–52)[c]	189 (176–204)	50 (37–85)	All 0				11 (8–11)
	3 mg/kg	1.1 (0.8–1.3)[c]	50 (30–56)	20 (9–24)[c]	222 (140–276)	66 (41–89)	All 0				6 (5–7)
	10 mg/kg	1.1 (1.0–1.4)[c]	71 (30–107)	12 (7–37)[c]	190 (183–206)	70 (46–85)	All 0				6 (5–7)
PC14PE6 ($N = 8$)	Control	N/A			558 (477–740)	86 (85–108)	65 (54–76)	N/A			N/A
	E7080										
	1 mg/kg				240 (208–311)[c]	77 (42–91)	20 (8–41)[c]				
	3 mg/kg				260 (206–285)[c]	79 (56–86)	19 (10–24)[c]				
	10 mg/kg				205 (195–232)[c]	69 (26–113)	11 (2–29)[c]				
H1048 ($N = 8$)	Control	1.6 (1.0–2.3)	77 (2–113)	24 (0–86)	N/A			490 (300–1,020)	52 (18–85)	40 (19–77)	6 (3–10)
	E7080										
	1 mg/kg	1.3 (1.0–1.7)	59 (17–122)	17 (4–25)				485 (310–670)	67 (52–83)	45 (33–63)	7 (4–9)
	10 mg/kg	0.9 (0.7–1.2)	33 (3–91)	6 (0–11)[c]				245 (200–450)[c]	47 (27–69)	15 (10–53)[c]	4 (0–6)[c]

Abbreviation: N/A, not applicable.

[a]Number of metastatic nodules larger than 2 mm in diameter.

[b]Median (range).

[c]$P < 0.05$.